Pharm Res (2013) 30:714–720
DOI 10.1007/s11095-012-0910-6

RESEARCH PAPER

Molecular Mobility as a Predictor of the Water Sorption by Annealed Amorphous Trehalose

Sunny P. Bhardwaj • Raj Suryanarayanan

Received: 28 June 2012 / Accepted: 11 October 2012 / Published online: 27 October 2012

ABSTRACT

Purpose The work aims at investigating the correlation of water sorption potential with different measures of molecular mobility in an annealed amorphous model compound (trehalose).

Methods Amorphous trehalose, prepared by freeze-drying, was annealed at 100°C (17°C < T_g) for up to 120 h. Global molecular mobility was studied using a broadband dielectric spectrometer in the frequency range of 10^6–10^{-2}Hz. Enthalpic recovery was measured by differential scanning calorimetry and water sorption profiles were obtained using an automated vapor sorption balance.

Results As a function of annealing time, there was an increase, both in average α-relaxation time and enthalpic recovery and a decrease in the amount of sorbed water. A strong linear correlation was observed between the water sorption potential and the dielectric relaxation time, indicating a common underlying mechanism of the effect of annealing time on these properties. Enthalpic recovery, which is widely used as a measure of structural relaxation, did not correlate well with the extent of water sorption.

Conclusions The α-relaxation time can be used as a predictor of the water sorption potential of amorphous trehalose. It will be of interest and value to develop such predictive models for other amorphous compounds of pharmaceutical interest.

KEY WORDS annealing · enthalpic recovery · molecular mobility · trehalose · water sorption

S. P. Bhardwaj · R. Suryanarayanan (✉)
Department of Pharmaceutics, University of Minnesota
Minneapolis, Minnesota 55455, USA
e-mail: surya001@umn.edu

S. P. Bhardwaj
Merck Research Laboratories, Merck & Co.
Rahway, New Jersey 07065, USA

INTRODUCTION

The physical form of the active pharmaceutical ingredient (API) in a solid dosage form can influence numerous properties of pharmaceutical interest including stability (physical and chemical) and *in vivo* performance of the dosage form. Traditionally, the thermodynamically stable crystalline form is preferred since it confers the highest stability. However, the majority of new drug candidates under development are characterized by such low aqueous solubility that, following oral administration, there is potential for incomplete absorption and therapeutic failure (1,2). This problem can be overcome by administering the drug in the amorphous state. This state confers higher apparent aqueous solubility (often orders of magnitude) and faster dissolution rate than its crystalline counterpart (3–6). However, the physicochemical stability of the amorphous form is a major challenge.

There is an additional potentially serious practical problem with the use of amorphous materials. The higher free energy of the amorphous state, responsible for the enhancement in solubility and dissolution rate, also results in an increased tendency to sorb water from the atmosphere. This is undesirable since water, with a glass transition temperature (T_g) of 135 K, plasticizes amorphous materials (7). In other words, water sorption lowers the T_g of the system and increases the molecular mobility which can increase the risk of physical (crystallization) as well as chemical instability (8–10). Therefore, it often becomes necessary to monitor and tightly control the water vapor pressure in the atmosphere, both during processing and storage of amorphous pharmaceuticals. However, practically, there are limits to the extent to which the water vapor pressure can be reduced, particularly during the manufacture and processing of pharmaceuticals. It is therefore highly desirable to reduce the water sorption potential of amorphous materials.

Amorphous materials, when stored at temperatures below but close to their T_g, undergo aging. Sub-T_g annealing (intentional aging) is known to cause a reduction in the sorption of soluble gases by glassy polymers and has been ascribed to a decrease in free volume (11,12). Similarly, annealing of trehalose caused a decrease in both the rate and extent of water sorption (13). Therefore, sub-T_g annealing of an amorphous compound can be an effective strategy to attenuate its water sorption tendency.

Since the molecular mobility is expected to be very slow below T_g, the risk of crystallization in a glass was believed to be negligible. However, several compounds have been reported to crystallize at temperatures substantially below their T_g's (14,15). Moreover, while crystallization below T_g may not occur in many cases, nucleation during annealing still remains a major concern. In an earlier study from our group, nucleation was found to be the reason for the decreased physical stability of annealed amorphous trehalose (13). Nucleation was also observed on sub-T_g annealing in frozen aqueous solutions of mannitol and trehalose (16). Therefore, while annealing is an approach to reduce the water sorption potential, prolonged annealing may result in nucleation which is undesirable. The effect of annealing on water sorption is very pronounced during the early stages of annealing (13). This effect becomes progressively less pronounced, as a function of annealing time. Thus prolonged annealing, in addition to the risk of increased crystallization propensity, does not offer any significant advantage in terms of reduction in water sorption. It is therefore valuable to investigate markers which can help predict the optimum annealing conditions to cause the desired decrease in the water sorption potential of amorphous materials.

A glassy material loses its excess enthalpy and free volume during annealing, leading to structural relaxation (17). The loss in enthalpy can be indirectly measured by differential scanning calorimetry (DSC) and is called enthalpic recovery. Structural relaxation also results in a reduction in global molecular mobility leading to an increase in the average relaxation time (18,19). We determined the effect of annealing on enthalpic recovery (by DSC) and dielectric relaxation time (by DDS) of amorphous trehalose. Our objective was to correlate the water sorption potential with these two measures of structural relaxation. It is expected that the coupled properties would exhibit similar annealing time dependence. In addition to conferring predictive capabilities for water sorption potential, this will also improve our understanding of the origin of these processes.

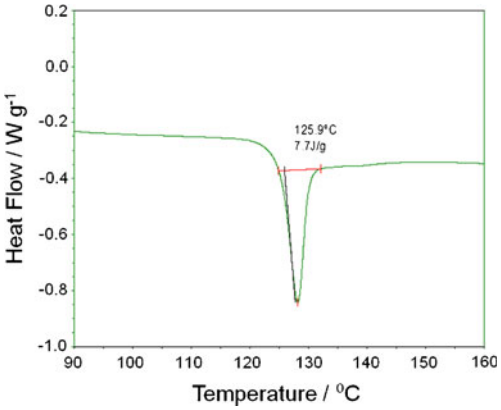

Fig. 2 DSC heating curve of amorphous trehalose annealed for 72 h.

MATERIALS AND METHODS

Preparation, Baseline Characterization and Annealing of Amorphous Trehalose

A 10% w/v aqueous solution of trehalose (α,α-trehalose dihydrate ($C_{12}H_{22}O_{11}{\cdot}2H_2O$); Sigma, St. Louis, MO, USA; purity > 99%) was freeze-dried using the procedure described earlier (20). Freeze-dried trehalose so obtained was X-ray amorphous and the water content was < 0.5% w/w (determined by Karl Fischer titrimetry and thermogravimetry). The amorphous trehalose was annealed at 100°C (~17°C < T_g) in a forced-air convection oven for up to 120 h. Aliquots, at selected time intervals, were subjected to water sorption, DSC and

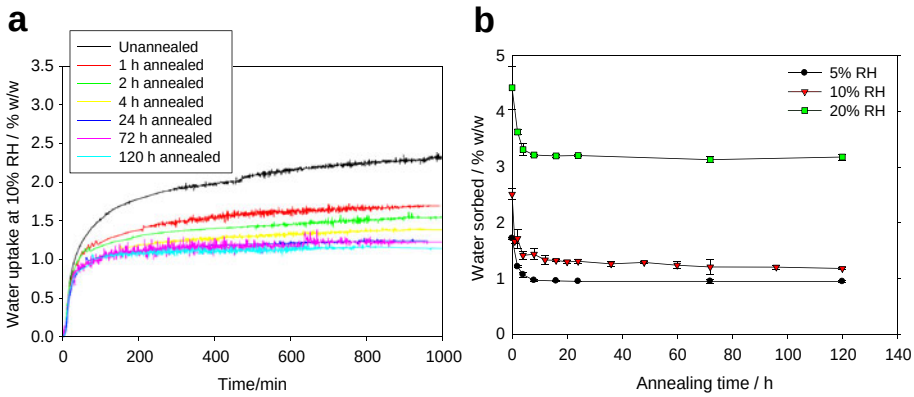

Fig. 1 (**a**) Kinetics of water sorption (at 10% RH) by amorphous trehalose annealed at 100°C for different time periods; (**b**) amount of water sorbed by amorphous trehalose as a function of annealing time when stored at 5, 10 or 20% RH (mean ± SD; n=3). The water sorption experiments were conducted at 25°C.

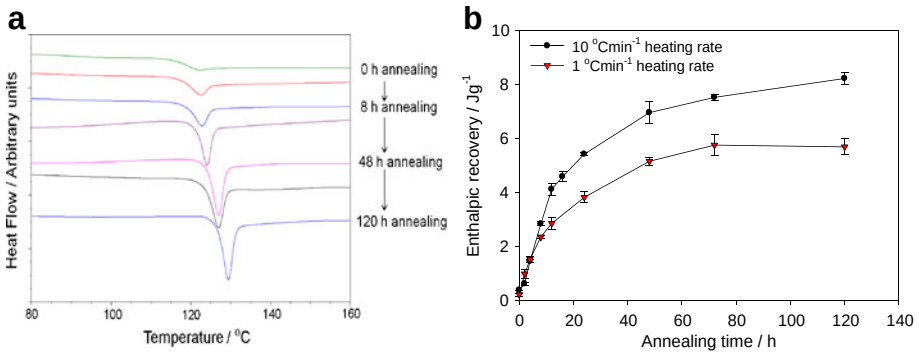

Fig. 3 (**a**) DSC heating curves (conventional DSC mode) of amorphous trehalose annealed at 100°C for different time periods, and (**b**) enthalpic recovery values as a function of annealing time obtained at two heating rates in DSC. Mean ± SD; n=3.

dielectric measurements. All the sample handling was done in a glove box maintained at RH < 5% (RT).

Thermal Analysis

A differential scanning calorimeter (Q2000, TA instruments, New Castle, DE, USA) equipped with a refrigerated cooling accessory was used. The cell constant was determined using indium and temperature calibration was performed using indium, tin and water as standards. In a glove box, the powder was hermetically sealed in aluminum pans. All the measurements were done under dry nitrogen purge at two different heating rates of 1 and 10°C/min.

Water Vapor Sorption

An automated vapor sorption balance (DVS-1000, Surface Measurements Systems, London, UK) was used. The microbalance was calibrated using a 100 mg standard weight. The relative humidity sensor was calibrated at 5.0, 11.3, 32.8, 52.8, 75.3, and 84.3% RH (25°C), using saturated salt solutions. About 6–8 mg of the sample was placed in the sample pan, dried at ~ 0% RH (dry nitrogen, at a flow rate of 200 ml/min) for 1,000 min, and then exposed to the desired RH. The extent of water uptake was determined at 5, 10 and 20% RH (25°C). The attainment of equilibrium was assumed when the weight change of the sample was < 0.0001% in 10 min.

Dielectric Spectroscopy

Using a broadband dielectric spectrometer (Novocontrol Alpha-A high performance frequency analyzer, Novocontrol Technologies, Germany), isothermal dielectric measurements were conducted at 100°C over the frequency range of 10^{-2} to 10^{6} Hz. The experimental details were presented earlier (20). The Havriliak-Negami function (Eq. 1) was used to fit the dielectric data so as to obtain the average relaxation time (τ) and shape parameters (β_{HN} and γ_{HN}).

$$\varepsilon^*(\omega) = \varepsilon_\infty + \frac{\Delta\varepsilon}{\left(1 + (i\omega\tau_{HN})^{\beta_{HN}}\right)^{\gamma_{HN}}} \quad (1)$$

$$\varepsilon^*(\omega) = \varepsilon'(\omega) - i\varepsilon''(\omega) \quad (2)$$

where, ω is the angular frequency which is equal to $2\pi f$ with f being the frequency in Hz, $\varepsilon^*(\omega)$ is the complex dielectric permittivity (Eq. 2) consisting of real (ε') and imaginary (ε") components, and dielectric strength, $\Delta\varepsilon=\varepsilon_s-\varepsilon_\infty$, where ε_s gives the low frequency limit ($\omega\rightarrow 0$) of $\varepsilon'(\omega)$ and ε_∞ is the high frequency limit ($\omega\rightarrow\infty$) of $\varepsilon'(\omega)$. The shape parameters

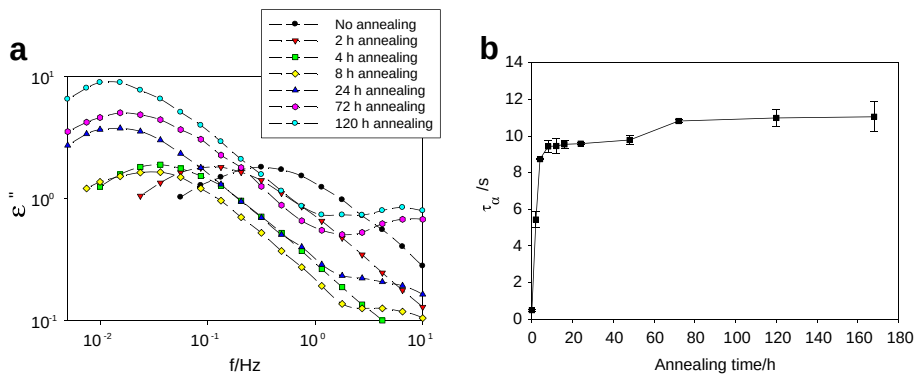

Fig. 4 (**a**) Isothermal dielectric loss spectra at 100°C of amorphous trehalose annealed at 100°C for different time periods; (**b**) plot of average α-relaxation time at 100°C as a function of annealing time. Mean ± SD; n=3.

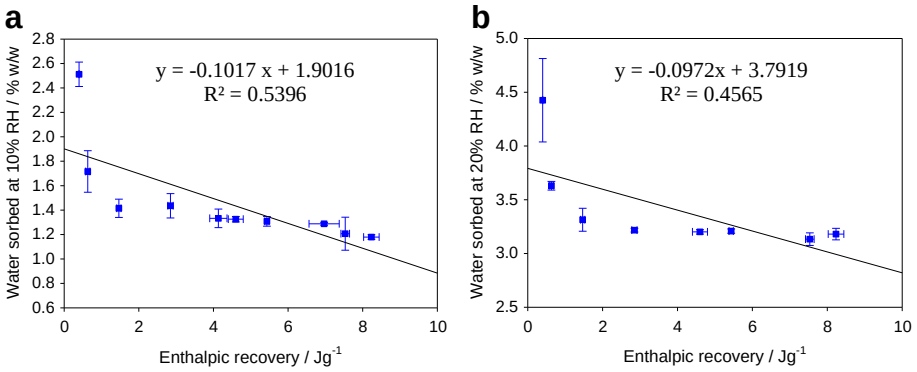

Fig. 5 Plots of amount of water sorbed at (**a**) 10% RH and (**b**) 20% RH *versus* enthalpic recovery. The enthalpic recovery was determined by DSC, at a heating rate of 10°C/min. Each data point corresponds to an annealing time point. *Lines* are linear regression fits to the data. Mean ± SD; $n=3$.

account for the symmetric and asymmetric peak broadening respectively with $0<\beta$ (or γ)<1.

RESULTS AND DISCUSSION

Effect of Annealing on Water Sorption Potential and on Enthalpic Recovery

Under all the conditions studied, the amount of water sorbed by trehalose decreased with annealing. As mentioned earlier, annealing is known to cause a reduction in the sorption potential of a glass (11–13). Figure 1a shows the water sorption profiles at 10% RH (25°C) and the effect of annealing is readily apparent. Interestingly, the effect of annealing is very pronounced in the first 4 h. Further annealing had only a small effect, if any, on reducing the amount of water sorbed at 10% RH. This is better shown in Fig. 1b where the amount of water sorbed is plotted as a function of annealing time. When a glass is stored at temperatures below but close to its T_g, it loses excess enthalpy and there is also a reduction in its free volume. Our water sorption results suggest that the decrease in free volume brought about during the first 4 h of annealing had the greatest influence on the water sorption capacity.

When an annealed glass is heated above its T_g, it recovers the lost enthalpy, manifested as an endotherm following the glass transition event in the DSC (Fig. 2). The experimental conditions can have a pronounced effect on the enthalpic recovery values. An increase in the DSC heating rate resulted in higher enthalpic recovery values (21). Therefore, we measured enthalpic recovery at heating rates of 1 and 10°C/min. There was a progressive increase in the enthalpic recovery as a function of annealing time (Fig. 3a; heating rate of 10°C/min). This effect was pronounced in the first 24 h of annealing at both the heating rates (Fig. 3b). As expected, an increase in heating rate resulted in higher enthalpic recovery values. This difference was particularly evident at longer annealing times. Both these observations are in agreement with the earlier report (21). However, the general trend was unaffected by the heating rate. Interestingly, unlike water sorption, annealing beyond 4 h continued to have a significant effect on enthalpic recovery.

Effect of Annealing on Dielectric Relaxation

We had recently used DDS to study the effect of annealing on the α-relaxation of trehalose (22). The samples were annealed and subjected to DDS at 100°C. Since there was considerable interference from dc conductivity, we used a derivative method of analysis based on the Kramers–Kronig relation to resolve and characterize α-relaxation (20,22). As shown in Fig. 4a, with increasing annealing time, the α-relaxation peak shifted to lower frequencies indicating an increase in structural relaxation time. The relaxation peak was modeled using the Havriliak-Negami equation so as to obtain the average relaxation time. When the α-relaxation time was plotted as a

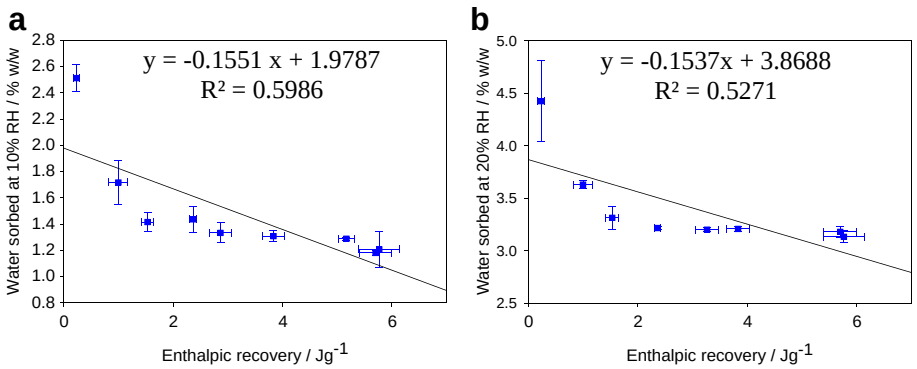

Fig. 6 Plots of amount of water sorbed at (**a**) 10% RH and (**b**) 20% RH *versus* enthalpic recovery. The enthalpic recovery was determined by DSC, at a heating rate of 1°C/min. Each data point corresponds to a unique annealing time. *Lines* are linear regression fits to the data. Mean ± SD; $n=3$.

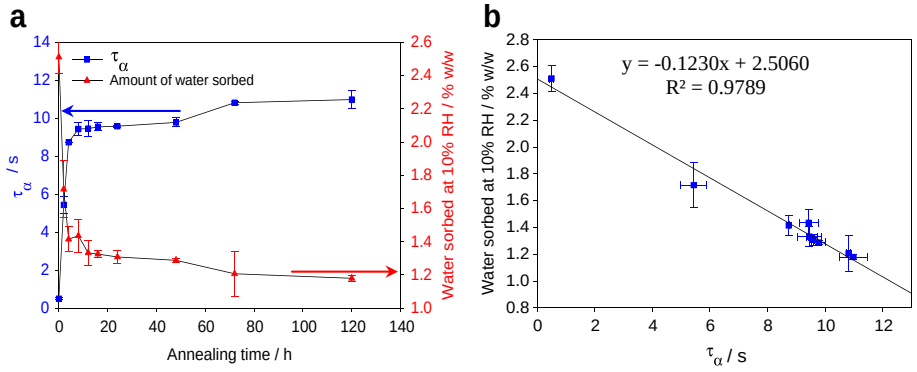

Fig. 7 (**a**) Plots of average *α*-relaxation time at 100°C (*left y-axis*) and amount of water sorbed (*right y-axis*) as a function of annealing time; and (**b**) plot of amount of water sorbed at 10% RH *versus* average *α*-relaxation time at 100°C; each data point corresponds to a unique annealing time and the *line* is the linear regression fit to the data. Mean ± SD; *n*=3.

function of annealing time, a sharp increase was observed in the first 4 h of annealing (Fig. 4b). Thereafter, the change in α-relaxation was much less pronounced. This shows that much like water sorption, the effect of annealing on dielectric relaxation was most pronounced in the first 4 h of annealing.

Correlation of Water Sorption with Enthalpic Recovery and *α*-relaxation Time

As mentioned earlier, annealing decreased the amount of water sorbed by trehalose. Our objective was to identify the property that can be used to predict this reduction in water sorption potential. To develop this predictive model, we investigated the correlation of water sorption with each enthalpic recovery and average *α*-relaxation time. At every annealing time, the amount of water sorbed was plotted against each of these quantities.

Figure 5a shows the correlation plot between the amount of water sorbed (10% RH; 25°C) and the enthalpic recovery (heating rate of 10°C/min). A similar profile was obtained following water sorption at 20% (Fig. 5b) and 5% RH (data not shown). It is evident that these two properties are not linearly correlated. Similar results were obtained at a lower heating rate of 1°C/min (Fig. 6). The effect of annealing on water sorption was most pronounced in the first 4 h of annealing, with longer annealing times having very little influence (Fig. 1b). On the other hand, the effect of annealing on enthalpic recovery persisted for a much longer time period.

As mentioned earlier, the first 4 h of annealing caused a sharp rise in the average *α*-relaxation time (Fig. 4b). The *α*-relaxation time as a function of annealing time is plotted in Fig. 7a. In the same figure, the amount of water sorbed (at 10% RH) is also plotted as a function of annealing time. The effect of annealing time on these two properties appears to be quite similar. One possible explanation is that the decrease in free volume brought about by annealing affects the rotational cooperative motions and water sorption in a similar way.

Finally, for each of these annealing times, a plot of amount of water sorbed *versus* the *α*-relaxation time revealed a linear correlation. Figures 7b and 8 are representative examples of the amount of water sorbed at 10 and 20% RH respectively. A similar correlation was observed at all the RH conditions employed. This indicates that the dielectric relaxation time can be used to predict the effect of annealing on the water sorption by trehalose. For most materials, structural relaxation is very slow in the sub-T_g region. As a result, frequency-domain dielectric measurements are impractically long. In such cases, time-domain dielectric spectroscopy is a better technique which has been traditionally used to study global mobility in the glassy state and also the effect of annealing on this relaxation (18,19). However, fast relaxation dynamics in glassy trehalose enabled us to use the frequency domain technique to evaluate the effect of annealing on *α*-relaxation.

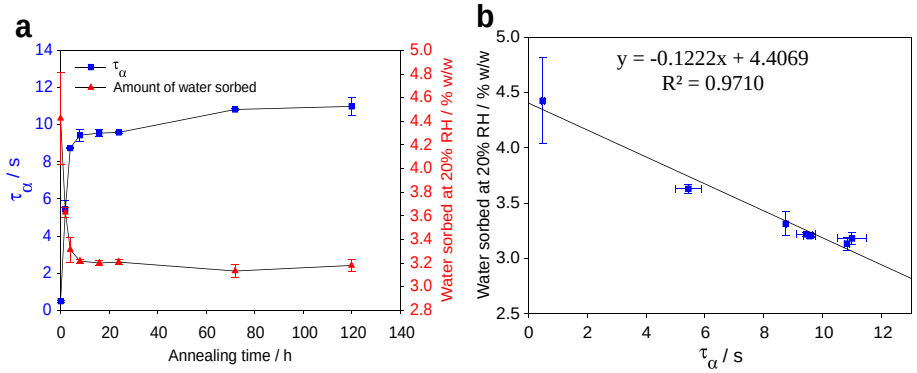

Fig. 8 Plots of (**a**) average *α*-relaxation time at 100°C (*left y-axis*) and amount of water sorbed (*right y-axis*) at 20% RH as a function of annealing time, and (**b**) amount of water sorbed at 20% RH *versus* average *α*-relaxation time at 100°C; each data point corresponds to a unique annealing time and the line is the linear regression fit to the data. Mean ± SD; *n*=3.

The dielectric relaxation time and enthalpic recovery responded very differently to sub-T_g annealing. Annealing was expected to have a substantially similar effect on these two properties, which are believed to be a consequence of the same underlying process of structural relaxation. However, in glassy trehalose, there may be decoupling of the dielectric and enthalpic relaxation processes. While dielectric spectroscopy measures mainly the rotational molecular motions, the enthalpic recovery measured by DSC is expected to be a consequence of multiple molecular motions in the material. This suggests that there is decoupling between rotational and translational motions which points towards the heterogeneous nature of trehalose glass. Such decoupling has been reported even in the supercooled liquid region of some compounds, although at temperatures close to T_g (17,23–25).

In amorphous trehalose, annealing seems to be affecting dielectric mobility and enthalpy of the system differently which leads to the above mentioned differences in the effect of annealing on enthalpic recovery and dielectric relaxation time. Moreover, based on the linear correlation between the dielectric relaxation time and amount of water sorbed at a particular RH, it seems that dielectric mobility (mainly rotational motions) is linked to the water sorption potential. Since a majority of pharmaceuticals are inherently heterogeneous in nature, such behavior is expected to be widespread. However, this might not be a universal phenomenon and in materials where there is no decoupling, enthalpic recovery should also be linearly correlated with water sorption.

CONCLUSIONS

On sub-T_g annealing, there was a decrease, both in global mobility (increase in average α-relaxation time) and water sorption, and an increase in enthalpic recovery. The amount of water sorbed decreased linearly with an increase in relaxation time. Thus dielectric measurements can potentially be used to predict the water sorption potential of amorphous materials. Interestingly, we did not observe such a correlation between water sorption and enthalpic recovery. Sub-T_g annealing, by slowing down molecular mobility and decreasing the tendency for water sorption, can be an effective strategy to stabilize amorphous materials.

ACKNOWLEDGMENTS AND DISCLOSURES

We are grateful to Brad L. Givot (3M, St. Paul, MN) for all his help in the dielectric measurements and 3M (St. Paul, MN) for providing us access to the dielectric spectrometer. We thank Vishard Ragoonan, Ph.D. and Khushboo Kothari for their comments. Partial support was provided by the William and Mildred Peters Endowment Fund.

REFERENCES

1. Nagapudi K, Jona J. Amorphous active pharmaceutical ingredients in preclinical studies: preparation, characterization, and formulation. Curr Bioact Compd. 2008;4:213–24.
2. Amidon GL, Lennernaes H, Shah VP, Crison JR. A theoretical basis for a biopharmaceutic drug classification: the correlation of *in vitro* drug product dissolution and *in vivo* bioavailability. Pharm Res. 1995;12:413–20.
3. Hancock BC, Zografi G. Characteristics and significance of the amorphous state in pharmaceutical systems. J Pharm Sci. 1997;86:1–12.
4. Craig DQM, Royall PG, Kett VL, Hopton ML. The relevance of the amorphous state to pharmaceutical dosage forms: glassy drugs and freeze dried systems. Int J Pharm. 1999;179:179–207.
5. Murdande SB, Pikal MJ, Shanker RM, Bogner RH. Solubility Advantage of Amorphous Pharmaceuticals: I. A Thermodynamic Analysis. J Pharm Sci. 2010;99:1254–64.
6. Murdande SB, Pikal MJ, Shanker RM, Bogner RH. Solubility advantage of amorphous pharmaceuticals: II. Application of quantitative thermodynamic relationships for prediction of solubility enhancement in structurally diverse insoluble pharmaceuticals. Pharm Res. 2010;27:2704–14.
7. Hallbrucker A, Mayer E, Johari GP. Glass transition in pressure-amorphized hexagonal ice. A comparison with amorphous forms made from the vapor and liquid. J Phys Chem. 1989;93:7751–2.
8. Hancock BC, Zografi G. The relationship between the glass transition temperature and the water content of amorphous pharmaceutical solids. Pharm Res. 1994;11:471–7.
9. Andronis V, Yoshioka M, Zografi G. Effects of sorbed water on the crystallization of indomethacin from the amorphous state. J Pharm Sci. 1997;86:346–51.
10. Yoshioka S, Aso Y. Correlations between molecular mobility and chemical stability during storage of amorphous pharmaceuticals. J Pharm Sci. 2007;96:960–81.
11. Chan AH, Paul DR. Influence of history on the gas sorption, thermal, and mechanical properties of glassy polycarbonate. J Appl Polym Sci. 1979;24:1539–50.
12. Chan AH, Paul DR. Effect of sub-T_g annealing on gas transport in polycarbonate. J Appl Polym Sci. 1980;25:971–4.
13. Surana R, Pyne A, Suryanarayanan R. Effect of aging on the physical properties of amorphous trehalose. Pharm Res. 2004;21:867–74.
14. Andronis V, Zografi G. Crystal nucleation and growth of indomethacin polymorphs from the amorphous state. J Non-Cryst Solids. 2000;271:236–48.
15. Li Y, Han J, Zhang GGZ, Grant DJW, Suryanarayanan R. *In situ* dehydration of carbamazepine dihydrate: a novel technique to prepare amorphous anhydrous carbamazepine. Pharm Dev Technol. 2000;5:257–66.
16. Pyne A, Surana R, Suryanarayanan R. Crystallization of mannitol below Tg' during freeze-drying in binary and ternary aqueous systems. Pharm Res. 2002;19:901–8.
17. Angell CA, Ngai KL, McKenna GB, McMillan PF, Martin SW. Relaxation in glassforming liquids and amorphous solids. J Appl Phys. 2000;88:3113–57.
18. Alegría A, Goitiandia L, Tellería I, Colmenero J. Dielectric relaxation and physical aging in polar glassy polymers. J Non-Cryst Solids. 1991;131–133:457–61.
19. Alegría A, Goitiandía L, Tellería I, Colmenero J. α-relaxation in the glass-transition range of amorphous polymers. 2. Influence of physical aging on the dielectric relaxation. Macromolecules. 1997;30:3881–7.

20. Bhardwaj SP, Suryanarayanan R. Subtraction of DC conductivity and annealing: approaches to identify Johari-Goldstein relaxation in amorphous trehalose. Mol Pharm. 2011;8:1416–22.
21. Surana R, Pyne A, Rani M, Suryanarayanan R. Measurement of enthalpic relaxation by differential scanning calorimetry-effect of experimental conditions. Thermochim Acta. 2005;433:173–82.
22. Bhardwaj SP, Suryanarayanan R. Use of dielectric spectroscopy to monitor molecular mobility in glassy and supercooled trehalose. J Phys Chem B. 2012;116:11728–36.
23. Cicerone MT, Ediger MD. Enhanced translation of probe molecules in supercooled o-terphenyl: signature of spatially heterogeneous dynamics? J Chem Phys. 1996;104:7210–8.
24. Cicerone MT, Blackburn FR, Ediger MD. Anomalous diffusion of probe molecules in polystyrene: evidence for spatially heterogeneous segmental dynamics. Macromolecules. 1995;28:8224–32.
25. Cicerone MT, Wagner PA, Ediger MD. Translational diffusion on heterogeneous lattices: a model for dynamics in glass forming materials. J Phys Chem B. 1997;101:8727–34.